Eur Arch Psychiatry Clin Neurosci (2013) 263:41–52
DOI 10.1007/s00406-012-0328-5

ORIGINAL PAPER

Astrocyte decrease in the subgenual cingulate and callosal genu in schizophrenia

Matthew Roy Williams · Thomas Hampton · Ronald KB Pearce · Steven Richard Hirsch · Olaf Ansorge · Maria Thom · Michael Maier

Received: 8 November 2011 / Accepted: 5 May 2012 / Published online: 4 June 2012

Abstract Decreases in glial cell density and in GFAP mRNA in the anterior cingulate cortex have been reported in schizophrenia, bipolar disorder and major depressive disorder. Our study examines astrocyte and oligodendrocyte density in the white and grey matter of the subgenual cingulate cortex, and at the midline of the genu of the corpus callosum, in schizophrenia, bipolar disorder, depression and normal control cases. Serial coronal sections were stained with H and E for anatomical guidance, cresyl haematoxylin for oligodendrocyte identification and GFAP immunohistochemistry for astrocyte identification. Oligodendrocyte and astrocyte density was measured using systematic anatomical distinctions and randomised counting methods. A significant decrease in astrocyte density was observed in schizophrenia compared with normal controls in the cingulate grey matter, cingulate white matter and the midline of the corpus callosum ($p = 0.025$). Bipolar disorder and depression cases showed no significant changes in astrocyte density. Oligodendrocytes did not show any changes between diagnostic groups. In subgenual cingulate cortex, the ratio of oligodendrocytes to astrocytes was decreased between the controls and the three disease groups, suggesting a specific glial cell type specific change in schizophrenia.

Keywords Schizophrenia · Cingulate · Astrocytes · Neuropathology

M. R. Williams (✉) · T. Hampton · R. K. Pearce · S. R. Hirsch · M. Maier
Neuropathology Unit, Department of Experimental Medicine, Imperial College London, Charing Cross Hospital, London W6 8RF, UK
e-mail: Matthew.r.williams@imperial.ac.uk

O. Ansorge
Department of Neuropathology, The Radcliffe Infirmary, Oxford OX2 6HE, UK

M. Thom
UCL, Institute of Neurology, Queen Square WC1N 3BG, UK

Introduction

Schizophrenia (SZ) is a serious psychiatric disorder characterised by positive symptoms such as auditory hallucinations, delusions and thought disorder affecting approximately 1 % of the world population. Cases of SZ, bipolar disorder (BPD) and major recurrent depressive disorder (MDD) were studied against matched controls to examine astrocyte and oligodendrocyte density in the grey and white matter regions of the subgenual cingulate cortex (SCC) and in the midline of the subgenual corpus callosum.

The anterior cingulate cortex (ACC) lies on the medial surface of the cerebral hemisphere, covering the anterior part of the corpus callosum. It is defined as Broadmann area 24a. The ACC extends from the subgenual ventral terminus and continues rostral to the genu of the corpus callosum following the dorsal surface. The ACC has been implicated in the regulation of emotional states and in cognitive and attentional processes [1, 6, 8, 9, 13]. The SCC white matter (WM) is made of projections directly from the SCC cortical grey matter (GM) to the corpus callosum. DTI studies have demonstrated decreased anisotropy in the cingulum bundle in patients with chronic SZ [23, 31].

The SCC shows lower activity in schizophrenia than controls during colour-incongruent testing, consistent with a decreased metabolic rate in schizophrenia, and lesions of the ventromedial prefrontal cortex result in an inability to

react emotionally to significant stimuli [1, 9, 18, 35]. A decrease in SCC glucose metabolism has been observed in MDD and BPD during the depressed phase [14]. Subgenual prefrontal cortex is decreased in volume (19 %) on the left side in females with adolescent onset depression, and also in MDD and unmedicated chronic BPD [4, 14].

Whilst stereological examination shows no change in overall volume in frontal cortices in schizophrenia [21, 34], cortical thinning has been observed in area 24a in both SZ and bipolar disorder (BPD) [5], and a decrease in the grey matter density in schizophrenia has also been reported in the orbitofrontal, cingulate and supramarginal cortices [19].

Neuropathological examination of post-mortem tissue in these psychiatric disorders has produced contradictory findings, conflicting reports of neuron density in the ACC in SZ. Both increase and decrease in ACC neuron density have been published [10, 12]. There has been reported a decrease in interneurons in layer II of the cingulate cortex in schizophrenia, together with an increase in GABA inhibitory interneurons [2, 22]. In both SZ and BPD, a lower neuron density in the ACC has been reported, particularly in the non-pyramidal neurons of layer I. Whilst neuron size is decreased in the orbitofrontal cortex in both BPD and MDD [5, 11, 30]. A decrease in neuron soma size has been shown in BPD, SZ and MDD [10].

Glial cells in the cingulate cortex have been reported to be reduced in number in SZ, BPD and MDD [12, 25]. This is consistent with changes in astrocytes in the prefrontal cortex in SZ, BPD and MDD [3, 24, 26, 32], although these findings are not universal [16]. Cingulate GFAP mRNA has been shown to be decreased in the ACC in SZ [33], and decreased synaptic markers in the subgenual region of the ACC have been reported [15]. Although more recently the spatial distribution and density of oligodendrocytes in the SCC WM have been shown to be unaltered in schizophrenia [29].

These findings suggest that a complex and diverse role of the ACC and, specifically, the SCC in severe mental illness.

Methods

Cases

Tissue was taken from the Corsellis brain collection, held by the West London Mental Health Trust, UK.

Coronal blocks containing SCC and anterior corpus callosum were obtained from 67 subjects, consisting of 20 cases with no history of psychiatric disorder (NPD), 11 SZ, 16 BPD and 20 MDD as diagnosed fulfilling ICD-10 criteria for diagnosis based upon medical notes held in the collection.

Documented cases involving alcohol or drug abuse or a concomitant neurological disorder were excluded from study. Cases were reviewed by a consultant neuropathologist to exclude significant pathology such as neurodegenerative diseases, cerebral vascular disease, ischaemic brain damage, CNS infections and all forms of dementia.

Tissue sampling

Bilateral SCC and anterior corpus callosum were removed from formalin-fixed coronal slices and immersed in 10 % formalin until processing (Fig. 1). Corpus callosum was not available in all cases (NPD $n = 14$, SZ $n = 4$, BPD $n = 10$, MDD $n = 16$). Processing involved serial immersion of tissue in formalin, alcohol, methanol and xylene for equal lengths during a 24-h period. Tissue blocks were then embedded in paraffin wax and chilled overnight at 4 °C. Paraffin-embedded blocks were serially sectioned in the coronal plane at a thickness of 10 μm, floated in warm water and mounted on 25 × 75 mm electrostatic glass slides. Cases were blinded by an investigator not involved with the project before staining and measurement.

Histology

For the grey matter profile, measurement adjacent sections were stained with cresyl violet by immersion in xylene for 30 min, incubated in 100, 90 and then 70 % alcohol for 10 min each, before immersion in ultra-pure water. Sections were immersed in cresyl violet stain for 5 min before washing in ultra-pure water and differentiation in 95 % alcohol/ethanoic acid. After washing in ultra-pure water, sections were dehydrated in serial alcohols, immersed in xylene and mounted with DPX.

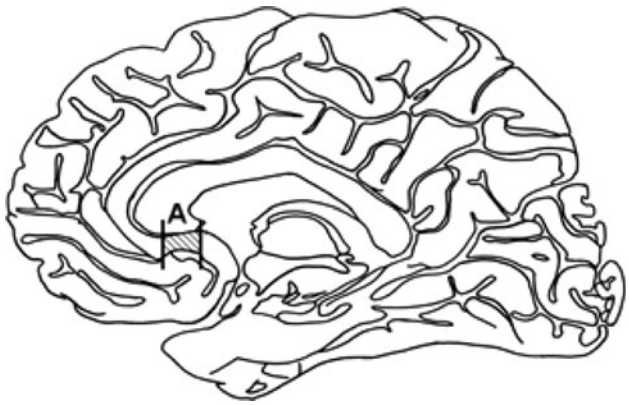

Fig. 1 Sagittal diagram illustrating the level of the coronal sampling the subgenual cingulate cortex (*shaded region A*)

Adjacent slides were stained for oligodendrocyte identification by double cresyl haematoxylin staining, performed by a standard cresyl stain as described previously, followed by washing in ultra-pure water, 3 min in 50 % Mayers haematoxylin solution, dehydration and mounting.

The thickness of layers I–VI were measured at the crown of the SCC, and at the mid-gyrus, defined as the area of grey matter halfway between the crown and the sulcus. Images were taken using an Olympus microscope at 40× and 100× magnification, at 2,096 × 1,536 resolution and measured using Image Pro Plus software (Media Cybernetics, US).

Immunohistochemistry

Paraffin-embedded 10 μm sections were immersed in xylene for 30 min, washed in double distilled water and followed by serial dehydration through 70, 90 and 100 % ethanol for 10 min each. Sections were immersed in methanol/3 % hydrogen peroxide solution for 30 min. Glial fibrillary acid protein (GFAP; Dako, ZO334) stained sections were boiled in 10 mM EDTA for 10 min for antibody retrieval and immediately placed in room temperature 0.1 M phosphate-buffered saline (PBS). Two hundred microlitres of primary antibody was added to each section, at a concentration GFAP 1:500 and incubated overnight at 4 °C. Sections were washed with 0.1 M PBS and secondary antibody solution (Dako, K5001) was added at 1:20 dilution for GFAP. Sections were incubated for 1 h at room temperature and washed. Sections were incubated at room temperature for 1 h with 200 μl ABC (Vector Labs, UK) solution. After PBS wash, sections were incubated with 3,3-diaminobenzene solution/1 % hydrogen peroxide solution for 3 min, followed by immersion in ultra-pure water. After washing for 10 min in running tap water, sections were immersed in stock Mayer's Haematoxylin for 5 s and washed in running tap water for 5 min. Sections were immersed in 70 % ethanol/1 % 1 M HCl for 3 s to differentiate. After 2 min washing in running tap water, sections were dehydrated in serial alcohols, immersed in xylene and mounted using DPX.

Image capture

Slides were placed under an Olympus microscope and images of regions of interest captured at 2,096 × 1,536 resolution at 4× magnification using Image Pro Plus. Images of 2,200 × 1,600 μm area were captured from the SCC crown and sulcus, the crown and base of the SCC white matter and the midline of the corpus callosum (see Fig. 2). The midline was chosen to avoid potential errors in identifying identical regions in the callosum between cases.

Identification of SCC grey matter layers

In the SCC, layer I was clearly defined with glial cells only present; layer II was primarily formed of small interneurons, typically smaller than layers I and III; layer III was well defined and contained pyramidal cells, less dense than either layers II or IV; layer IV was similar to layer II; although typically thinner and containing a slightly lower neuron density; layer V was often well defined on the superficial margin, containing large pyramidal cells and characteristic spindle cells towards layer VI; layer VI was defined by an absence of pyramidal cells and a presence of large oval neurons on the boundary of layer V.

The crown of the SCC was measured at the midline of the gyral crown of the grey matter of the SCC consistent with the orientation of the neuronal columns projecting from the white matter to the superficial crown of the gyrus.

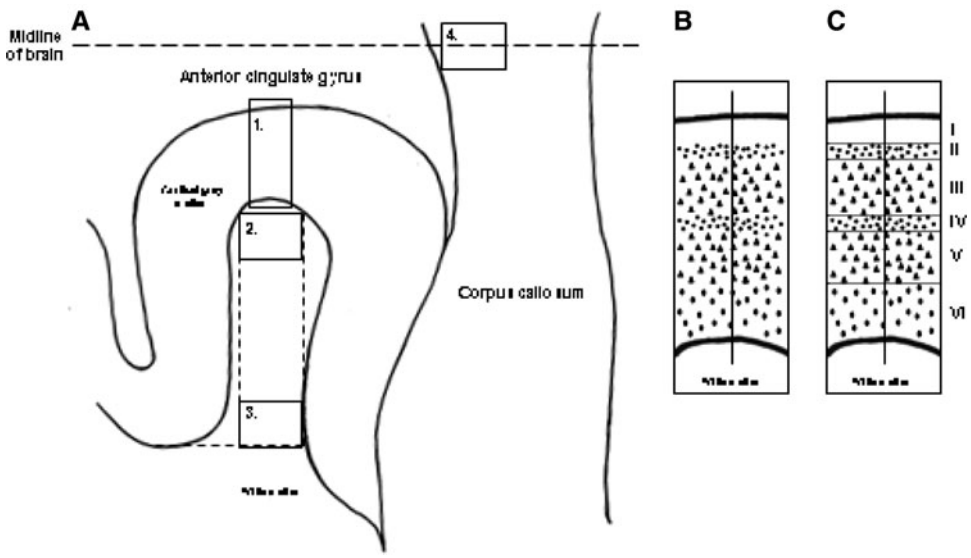

Fig. 2 **a** Coronal section through SCC and corpus callosum, rotated to show the gyrus in profile. The four regions measured are *1* grey matter from SCC crown, in total and by layers (see **b** and **c**). *2* Crown of gyral white matter. *3* Base of gyral white matter, adjacent to sulcal grey matter. *4* Midline of corpus callosum on outer surface. Brain midline is indicated. **b** Aligned images of grey matter at crown. **c** Division of cortical grey matter into layers prior to density measures

The thickness of the SCC cortical layers was measured using a calibrated tool within Image Pro Plus. These measurements were used to guide the thickness measurement on GFAP-stained slides along with the haematoxylin counterstain. A 1-mm-wide region from the crown of the SCC to the white matter was defined and the cortical layers mapped within. This process is illustrated in Fig. 2.

Glial cell identification

Astrocyte cell bodies were defined as a clearly GFAP-stained cell body containing a counterstained nucleus or showing clearly GFAP-stained projections and counted within these layers. Oligodendrocytes were defined as small, round, darkly stained cells 4–6 μm in diameter with clearly counterstained large nuclear structure.

Analysis of ACC white matter

For cell density analysis in the corpus callosum and white matter regions a grid of 11 × 8, 200 × 200 μm^2 was laid over each image. A random number generator (www.graphpad.com, Graphpad Softare, USA) was used to identify squares for cell counting. Cells were manually counted in ten of these random squares using definitions described previously to give density measurements by cell number in a total area of 400,000 μm^2 (see Fig. 3).

Cell counting accuracy

Cell counts were replicated in five randomly selected cases (cases 13, 16, 19, 46 and 64). A total of three repeat measures using identical methods were performed in these cases with at least 1 week between measures. This was performed by the primary investigator for intrarater accuracy, and a second investigator not involved with the project for inter-rater accuracy. The overall counting error rate was 7.4 % for intrarater measures, where the main investigator was assessed for accuracy, and 7.2 % for inter-rater measures.

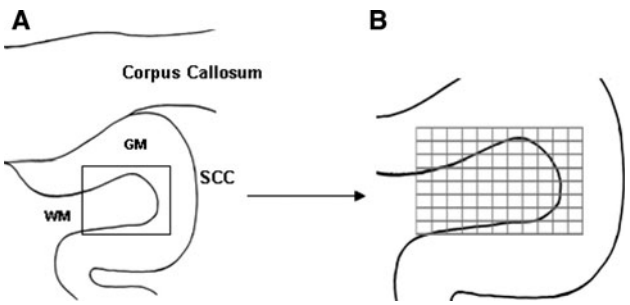

Fig. 3 Illustration of gird mask for random counting of white matter regions. **a** A region covering the region of the cortical white matter would be (**b**). An 88-square grid mask was imposed over the region, was numbered and randomly selected for counting as described in text. Randomly selected squares overlapping cortical grey matter, as observed by the presence of haematoxylin-stained neurons, were not used and new squares were selected for cell counting up to a total of 10 (total area of 400,000 μm^2)

Statistics

Measures were performed blind to diagnosis and were unblinded by an investigator not involved with the project before analysis using Image Pro Plus. Statistical analysis was performed in collaboration with a consultant statistician. Direct comparisons were analysed using a one-way ANOVA and two-tailed *t* tests. Multiple comparisons were performed using the general linear model univariate analysis (GLM) with Scheffe multiple comparisons, with age, sex and diagnosis as interacting variables. The potential confounding effects of age, PM delay and formalin fixation period were evaluated using multiple regression analysis with backward selection, within each diagnostic group and with combined groups. Analysis was performed using SPSS v14.0 statistical software (SPSS, USA).

Ethics

This project was conducted under ethical permission granted by the London south west local ethics committee reference WL/02/12 (2002), and amendment WL/02/12/AM01, granted by the Ealing and WLMHT local research ethics committee (2006).

Results

Group differences

The MDD group had a significantly lower age of death as compared to controls ($p = 0.038$, one-way ANOVA). The MDD group ($n = 11$) contained 11 confirmed cases of suicide. The other disease groups also showed instances of suicide, which may contribute towards the non-significant trend downward in age in SZ (one suicide, $n = 11$) and BPD (3 suicides, $n = 16$).

There was no difference in PM delay between groups ($p = 0.60$, one-way ANOVA), shown in Table 1. The BPD tissue had been stored in formalin significantly longer than the other diagnostic groups ($p < 0.001$, one-way ANOVA). Regression analysis showed no effect of formalin storage duration on density of astrocytes within the BPD group ($r^2 = 0.038$, $p = 0.23$) or overall ($r^2 = 0.007$, $p = 0.84$), or upon oligodendrocyte density within the BPD group ($r^2 = 0.033$, $p = 0.54$) or overall ($r^2 < 0.001$, $p = 0.81$).

Table 1 Summary of clinical and histological information on the brains from the Corsellis collection

Case no.	Corsellis code	Age/years	Sex	ICD10-diagnosis	PM delay/h	Time in formalin/years	CoD
1	12/95	69	M	NPD	10	8	Acute bronchiolitis
2	23/91	45	F	NPD	23	12	Diffuse non-Hodgkin's lymphoma
3	11/95	64	F	NPD	31	8	Coronary thrombosis
4	33/95	75	M	NPD	42	8	Malignant neoplasm of bladder
5	43/95	56	M	NPD	5	8	Coronary thrombosis
6	37/90	68	M	NPD	66	13	Multiple myeloma
7	65/95	64	M	NPD	101	8	Congestive heart failure
8	22/90	76	M	NPD	NK	13	Pneumonia
9	5/95	48	M	NPD	25	8	Coronary thrombosis
10	10/95	61	F	NPD	48	8	Myocardial infarction
11	34/95	58	F	NPD	98	8	Chronic ischaemic heart disease
12	75/91	33	M	NPD	NK	12	Acute myocarditis
13	30/90	62	M	NPD	NK	13	Chronic ischaemic heart disease
14	14/95	70	M	NPD	34	8	Chronic ischaemic heart disease
15	57/90	77	F	NPD	29	13	Non-Hodgkin's lymphoma
16	15/91	82	F	NPD	30	12	Malignant neoplasm of breast
17	12/91	59	M	NPD	68	12	Pulmonary embolism
18	22/91	65	M	NPD	20	12	Septicaemia
19	14/91	82	F	NPD	77	12	Pneumonia
20	75/94	64	F	NPD	NK	9	Malignant neoplasm of breast
21	16/97	72	F	SZ	NK	6	Congestive heart failure
22	77/88	22	M	SZ	18	15	Intentional self-poisoning
23	5/97	80	F	SZ	50	6	Hepatic failure
24	40/94	80	F	SZ	75	9	Malignant neoplasm of colon
25	28/95	50	M	SZ	80	8	Pneumonia
26	28/94	50	F	SZ	40	9	Malignant neoplasm of lung
27	10/97	66	M	SZ	24	6	Myocardial infarction
28	63/90	50	F	SZ	NK	13	Hypothermia
29	27/88	34	M	SZ	NK	15	Pneumonia
30	76/91	66	M	SZ	NK	12	Chronic ischaemic heart disease
31	37/85	82	F	SZ	NK	18	NK
32	40/96	37	M	BPD	89	7	Multiple Injuries
33	113/81	79	M	BPD	51	22	Chronic ischaemic heart disease
34	228/74	49	M	BPD	91	29	Congestive heart failure
35	47/97	47	F	BPD	27	6	Intentional self-poisoning
36	388/77	64	F	BPD	12	26	Pneumonia
37	25/89	33	M	BPD	52	14	Suicide—explosive
38	67/75	55	F	BPD	28	28	Pulmonary embolism
39	2/89	63	F	BPD	58	14	Congestive heart failure
40	93/88	21	F	BPD	NK	15	Intentional self-poisoning
41	8/88	66	M	BPD	51	15	Myocardial infarction
42	31/90	58	M	BPD	NK	13	Pulmonary embolism
43	331/77	77	F	BPD	16	26	Congestive heart failure
44	105/72	77	F	BPD	36	31	Duodenal ulcer
45	105/86	63	M	BPD	100	17	Atherosclerosis
46	1/84	60	F	BPD	55	19	Congestive heart failure
47	48/80	64	F	BPD	42	23	Malignant neoplasm of breast
48	44/91	48	M	MDD	17	12	Suicide—CO

Table 1 continued

Case no.	Corsellis code	Age/years	Sex	ICD10-diagnosis	PM delay/h	Time in formalin/years	CoD
49	48/88	41	F	MDD	28	15	Intentional self-poisoning
50	21/88	48	F	MDD	47	15	Suicide—Jumping
51	72/96	52	M	MDD	53	7	Malignant neoplasm of oesophagus
52	100/88	60	F	MDD	NK	15	Pneumonia
53	61/90	54	M	MDD	7	13	Suicide—Burning
54	11/91	45	F	MDD	66	12	Intentional self-poisoning
55	14/97	32	F	MDD	39	6	Intentional self-poisoning
56	14/89	68	F	MDD	NK	14	Pneumonia
57	56/88	70	F	MDD	48	15	Pneumonia
58	17/97	32	F	MDD	39	6	Sudden death, cause unknown
59	20/97	44	F	MDD	41	6	Asphyxiation
60	6/97	35	M	MDD	50	6	Asphyxiation
61	15/97	53	M	MDD	26	6	Intentional self-poisoning
62	19/90	37	F	MDD	17	13	Suicide—CO
63	24/89	47	F	MDD	NK	14	Suicide—Hanging
64	26/97	42	M	MDD	26	6	Asphyxiation
65	21/91	65	F	MDD	20	12	Intentional self-poisoning
66	35/96	18	F	MDD	98	7	Intentional self-poisoning
67	1/87	79	F	MDD	7	16	Myocardial infarction

Diagnostic codes from ICD-10. *NPD* no psychiatric disorder, *SZ* schizophrenia, *BPD* bipolar disorder, *MDD* major depressive disorder. *NK* not known

Table 2 Summary group data

Diagnosis	(*n*)	Age/years	Sex ratio M/F	PM delay/h	Fixation time/years
NPD	19	65.5 (2.34)	11/8	44.2 (7.38)	10.2 (0.52)
SZ	10	58 (6.44)	5/5	47.8 (10.5)	11.1 (1.30)
BPD	15	56.1 (5.21)	6/9	50.5 (7.46)	19.4 (2.02
MDD	20	47.6 (3.12)	7/13	37.3 (5.62)	10.4 (0.88)

NPD no psychiatric disorder, diagnosis codes from ICD-10

Age, PM delay and fixation time shown as means with SEM in brackets. *NPD* no psychiatric disorder. *SZ* schizophrenia, *BPD* bipolar disorder, *MDD* major depressive disorder

The age of death also showed no relation to astrocyte density within the MDD group ($r^2 = 0.032$, $p = 0.47$) or overall ($r^2 = 0.013$, $p = 0.37$) and also showed no relation to the oligodendrocyte within the MDD group ($r^2 = 0.058$, $p = 0.33$) or overall ($r^2 = 0.001$, $p = 0.77$) (Table 2; Fig. 4).

SCC grey matter

The profile of astrocyte density across the cortical layers of the SCC shows a distinct pattern, with layers I and VI showing a significantly increased density compared with layers II–V (Fig. 5, $p < 0.050$, one-way ANOVA with Tukey's post hoc analysis for each diagnostic group).

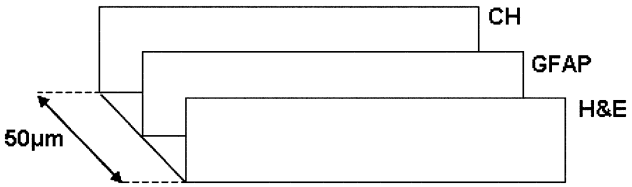

Fig. 4 Illustration of order of staining of sections from the *SCC*, with *H and E* being the most anterior. Stains were haematoxylin and eosin (*H&E*), Glial fibrillary acid protein immunohistochemistry (*GFAP*) and cresyl haematoxylin (*CH*). The three sections were cut within 50 µm of each other

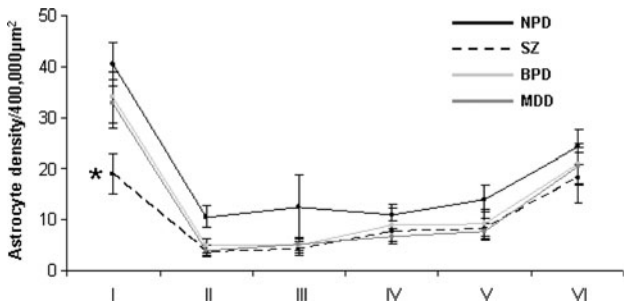

Fig. 5 Astrocyte density across the six cortical layers of the SCC GM. *NPD* no psychiatric disorder, $n = 19$, *SZ* schizophrenia, $n = 10$, *BPD* bipolar disorder, $n = 15$, *MDD* major depressive disorder, $n = 19$. Layer I astrocyte density in SZ decreased compared with the other diagnostic groups ($p < 0.050$) and to NPD ($p < 0.001$). Data shown as mean ± SEM

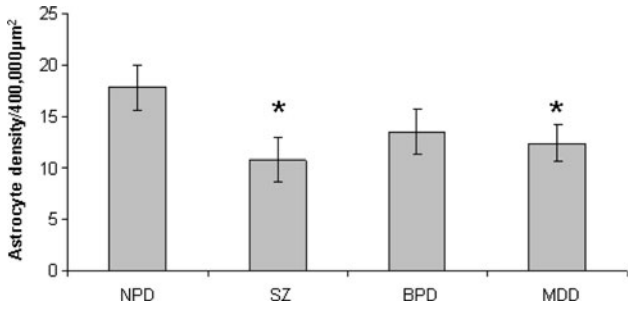

Fig. 6 Astrocyte density in whole SCC GM. *NPD* no psychiatric disorder, $n = 19$, *SZ* schizophrenia, $n = 10$, *BPD* bipolar disorder, $n = 15$, *MDD* major depressive disorder, $n = 19$. Astrocyte density is decreased in SZ and MDD groups ($p = 0.0022$). Data shown as mean ± SEM

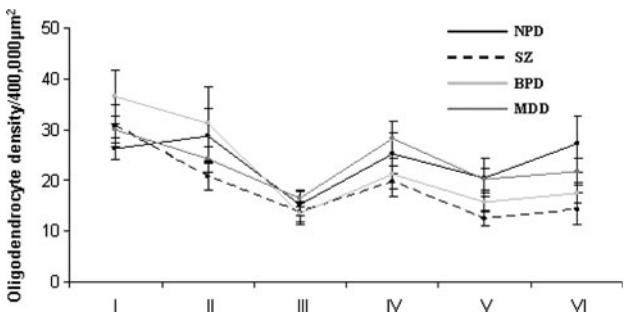

Fig. 7 Oligodendrocyte density across the six cortical layers of the SCC GM. *NPD* no psychiatric disorder, $n = 19$, *SZ* schizophrenia, $n = 10$, *BPD* bipolar disorder, $n = 15$, *MDD* major depressive disorder, $n = 19$. No difference between diagnostic groups was observed ($p = 0.926$). Data shown as mean ± SEM

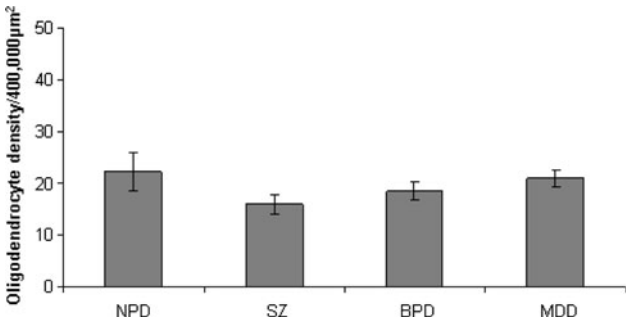

Fig. 8 Oligodendrocyte density over whole SCC GM. *NPD* no psychiatric disorder, $n = 19$, *SZ* schizophrenia, $n = 10$, *BPD* bipolar disorder, $n = 15$, *MDD* major depressive disorder, $n = 19$. No difference between diagnostic groups was observed ($p = 0.422$). Data shown as mean ± SEM

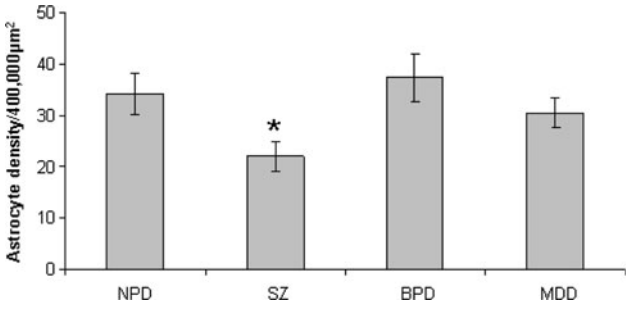

Fig. 9 Astrocyte density in SCC WM crown. *NPD* no psychiatric disorder, $n = 19$, *SZ* schizophrenia, $n = 10$, *BPD* bipolar disorder, $n = 15$, *MDD* major depressive disorder, $n = 19$. Astrocyte density is decreased in SZ compared to other diagnostic groups ($p < 0.050$). Data shown as mean ± SEM

Only layer I showed significant differences in astrocyte density between the diagnostic groups ($p = 0.009$, one-way ANOVA). The SZ group showed a lower density in layer I compared with the other disease groups ($p < 0.05$, GLM) and with the NPD controls ($p < 0.001$, one-way ANOVA with Tukey's post hoc analysis). The overall astrocyte density in the SCC grey matter was significantly decreased in SZ and MDD (Fig. 6, $p = 0.0022$, one-way ANOVA with Tukey's post hoc analysis).

There was no change in oligodendrocyte density by diagnosis across the profile of the SCC cortical layers (Fig. 7, $p = 0.926$, GLM) or overall (Fig. 8, $p = 0.422$, one-way ANOVA). There was no effect of sex or lateralisation on the astrocyte or oligodendrocyte density in the SCC grey matter.

SCC white matter

Overall, there was a significant effect of diagnosis on astrocyte density in the crown and base of the SCC WM and anterior corpus callosum ($p = 0.050$, GLM), where the schizophrenia group showed a significant effect of astrocyte density decreasing across the three white matter regions combined as compared with controls and the bipolar disorder group ($p = 0.025$, GLM with Scheffe multiple comparison). However, there was no any significant decrease in astrocyte density in any specific region.

The SCC WM crown showed a trend to decrease but no overall significant difference in astrocyte density (Fig. 9, $p = 0.080$, one-way ANOVA), but direct comparison of SZ with other diagnostic groups showed significant decrease (SZ 22.1 ± 3.00 v. NPD 34.4 ± 4.00, $p = 0.021$; SZ 22.1 ± 3.00 v. BPD 37.4 ± 4.56, $p = 0.005$; SZ 22.1 ± 3.00 v. MDD 30.61 ± 2.83, $p = 0.025$, *t* tests).

In the SCC WM base, significant changes were observed between the diagnostic groups in astrocyte density (Fig. 10, $p = 0.37$, one-way ANOVA). Direct comparison of SZ with NPD showed a decrease in astrocyte density in the base of the WM of the SCC (SZ 21.35 ± 4.19 v. NPD 31.75 ± 3.14, $p = 0.031$, *t* test), and SZ compared directly against BPD showed a trend towards decreased astrocyte

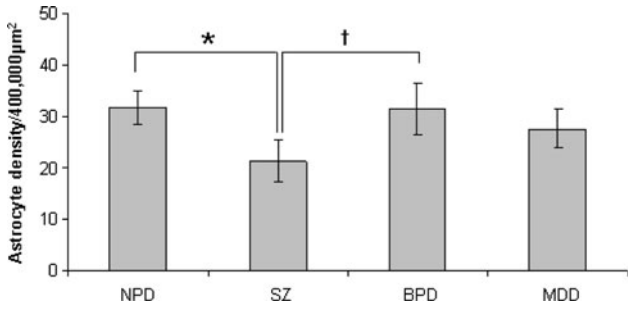

Fig. 10 Astrocyte density in SCC WM base. *NPD* no psychiatric disorder, $n = 19$, *SZ* schizophrenia, $n = 10$, *BPD* bipolar disorder, $n = 15$, *MDD* major depressive disorder, $n = 19$. Astrocyte density is decreased in SZ compared with NPD ($^{*}p < 0.050$), and a trend towards astrocyte decrease compared to BPD ($^{\dagger}p < 0.10$). Data shown as mean ± SEM

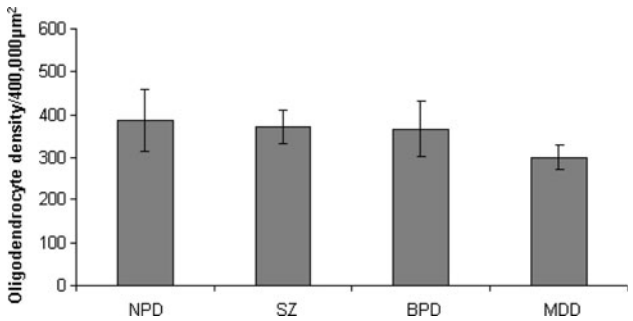

Fig. 11 Oligodendrocyte density in SCC WM crown. *NPD* no psychiatric disorder, $n = 19$, *SZ* schizophrenia, $n = 10$, *BPD* bipolar disorder, $n = 15$, *MDD* major depressive disorder, $n = 19$. No difference between diagnostic groups was observed ($p = 0.225$). Data shown as mean ± SEM

density (SZ 21.35 ± 4.19 v. BPD 31.47 SZ ± 4.95, $p = 0.065$, *t* test).

There was no change in oligodendrocyte density between diagnostic groups in either the SCC WM crown (Fig. 11, $p = 0.776$, one-way ANOVA) or SCC WM base (Fig. 12, $p = 0.225$, one-way ANOVA). In SCC WM base, direct comparison of SZ with NPD (SZ 343 ± 50 v. NPD 501 ± 34, $p = 0.053$, *t* test) and MDD with NPD (MDD 355 ± 44 v. NPD 501 ± 34, $p = 0.053$, *t* test) suggests a trend towards decreased oligodendrocyte density.

Anterior corpus callosum

Astrocyte density in the midline of the anterior corpus callosum shows no significant change overall ($p = 0.12$, one-way ANOVA), although direct comparison between diagnostic groups reveals a significant decrease in astrocyte density in SZ compared with NPD (Fig. 13, SZ 12.50 ± 11.12 v. NPD 31.57 ± 4.86, $p = 0.038$, *t* test).

Oligodendrocyte density showed no change between diagnostic groups in the anterior corpus callosum (Fig. 14, $p = 0.461$, one-way ANOVA).

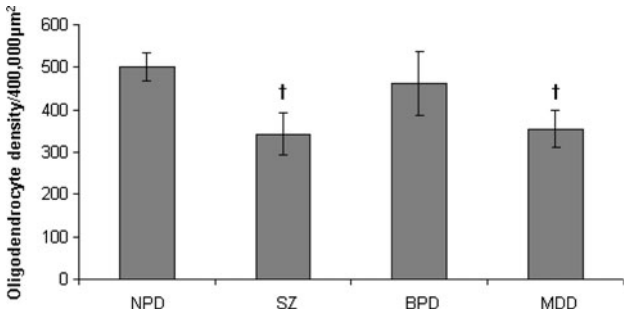

Fig. 12 Oligodendrocyte density in SCC WM base. *NPD* no psychiatric disorder, $n = 19$, *SZ* schizophrenia, $n = 10$, *BPD* bipolar disorder, $n = 15$, *MDD* major depressive disorder, $n = 19$ ($^{\dagger}p < 0.10$ compared with NPD). Data shown as mean ± SEM

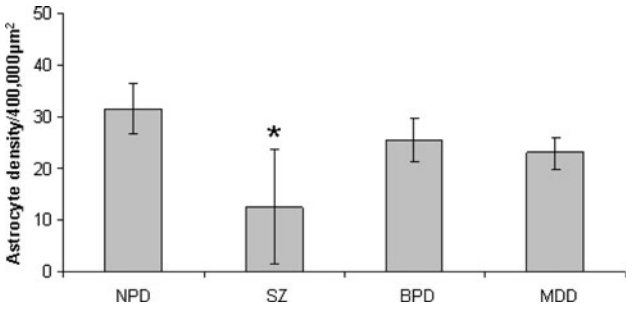

Fig. 13 Astrocyte density in anterior corpus callosum. *NPD* no psychiatric disorder, $n = 14$, *SZ* schizophrenia, $n = 4$, *BPD* bipolar disorder, $n = 10$, *MDD* major depressive disorder, $n = 16$ ($^{*}p < 0.050$). Data shown as mean ± SEM

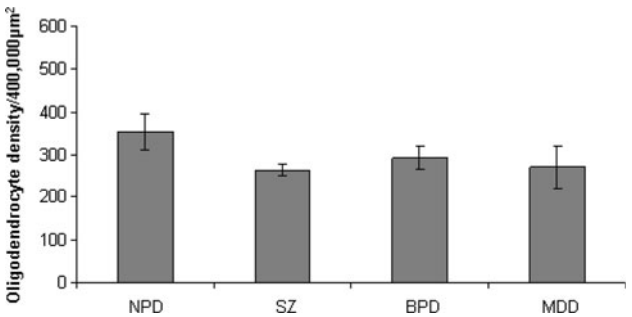

Fig. 14 Oligodendrocyte density in anterior corpus callosum. *NPD* no psychiatric disorder, $n = 14$, *SZ* schizophrenia, $n = 4$, *BPD* bipolar disorder, $n = 10$, *MDD* major depressive disorder, $n = 16$. Data shown as mean ± SEM

Relative number of glial subtypes

The ratio of oligodendrocyte to astrocyte density is shown in Table 3. The three WM regions show consistent ratios across all diagnostic groups. GM glial density ratio shows substantial drop for the SZ (112 oligodendrocytes, 61

Table 3 Relative mean number of oligodendrocytes and astrocytes

	GM			WM crown			WM base			Corpus callosum		
	Oligo	Astro	Ratio	Oligo	Astro	Ratio	Oligo	Astro	Ratio	Oligo	Astro	Ratio
NPD	143	13	11:1	386	34	11.4:1	501	32	15.7:1	354	32	11.1:1
SZ	112	61	1.84:1	372	22	16.9:1	343	21	16.3:1	262	13	20.2:1
BPD	136	83	1.64:1	367	37	9.9:1	462	31	14.9:1	292	26	11.2:1
MDD	141	80	1.76:1	300	31	9.8:1	355	28	12.7:1	270	23	11.7:1

Results are shown as means of cells/400,000 μm^2 averaged by group. *Oligo* oligodendrocyte number, *Astro* astrocyte number, *GM* cortical grey matter, *WM* white matter

astrocytes, 1.84:1), BPD (136 oligodendrocytes, 83 astrocytes, 1.64:1) and MDD (141 oligodendrocytes, 80 astrocytes, 1.76:1) groups as compared to NPD (143 oligodendrocytes, 13 astrocytes, 11:1).

Discussion

This study has three major findings. The most significant finding is the decrease in astrocyte, but not oligodendrocyte, density in the schizophrenia group as compared to the normal controls.

The ratio of oligodendrocytes to astrocytes decreases substantially in SCC grey matter in the three disease groups compared with controls and is elevated in the callosum in SZ.

Also, astrocyte density is significantly decreased in layer I of the SCC GM in SZ compared with other diagnostic groups.

These findings suggest a complex interaction of disease state and glial biology, with the glial subtypes showing different responses in the subgenual region in SZ, BPD and MDD.

Grey matter profile results

The data show that the density of astrocytes is decreased in the SCC grey matter in schizophrenia and depression. The bipolar disorder group exhibit a non-significant decrease. Previously, the total number of glia has been reported to decrease in the ACC of familial depression and bipolar disorder cases [25]. Our study does not make the distinction of familial and non-familial cases. We examine the different regions of the SCC, separating the grey matter and two regions of the white matter. The decrease in astrocyte density in depression is only found in the SCC grey matter, in contrast to white matter in schizophrenia, suggesting a different effect of these disease states on astrocytic migration. This data also reinforces the idea that the SCC is a vulnerable structure in mental illness generally.

The profile of astrocyte density across the crown of the SCC shows the highest density in layer I and VI, and a lower density in the other cortical layers in all four examined groups. The higher astrocyte density in layer VI is consistent with previously reported GFAP mRNA density in the ACC, but the high astrocyte density in layer I has not been previously reported [33]. Previously, GFAP mRNA was quantified using relative optical density measures from [35] S-labelled riboprobe in situ hybridization, a technique that is better for quantification than immunohistochemistry. GFAP immunohistochemistry is a proven method for identifying astrocyte cell bodies but is poor as a quantitative method for protein concentration. This may suggest that in the molecular layer of the SCC, there is a high density of astrocytes with a low expression of GFAP. GFAP has previously been suggested as a marker for astrocyte activation, and therefore, layer I astrocytes may be in an inactive state. The decrease observed in layer I astrocyte density in schizophrenia may reflect a change in the number of inactive astrocytes, but not an overall decrease in GFAP mRNA expression.

The lack of change oligodendrocyte density in SCC GM in schizophrenia is consistent with previous findings [25, 29]. As schizophrenia is often described a disorder of both function and connectivity, it is not necessarily expected that oligodendrocytes would not decrease, both as their role in maintaining axonal myelin would be one route of connective disruption if affected and with the reported expression decrease of myelin-related genes [17]. However, it may be that the activity, function or densities of oligodendrocytes are affected in schizophrenia, but simply not in the anterior cingulate or corpus callosum.

White matter results

Previous studies have shown no change in the density of GFAP-immunostained cells or labelling intensity, reflecting protein levels, in the deep white matter of schizophrenia cases as compared to controls [16, 27, 28]. In contrast astrocyte number in the prefrontal cortex, white matter has been reported to decrease in schizophrenia and

depression. GFAP mRNA levels in the white matter of the ACC decrease in both schizophrenia and bipolar disorder [32, 33].

In schizophrenia, there is an overall decrease in astrocyte density across the three examined regions. The difference in astrocyte densities observed across the two regions of SCC white matter examined, and the similar profiles observed between the crown and base of the SCC white matter, is more pronounced in the crown of the SCC white matter.

A decrease in astrocyte density is also observed in the midline of the anterior corpus callosum in the schizophrenia group; however, due to previous sampling, the corpus callosum was not available in all cases. The decrease is significant by direct *t* test between schizophrenia and controls, but not by ANOVA. This could well be a real finding, the sample size of four schizophrenia cases and the large SEM in this sample means some scepticism should be employed, and this finding repeated by other researchers for confirmation.

A lack of change in oligodendrocyte density in schizophrenic SCC WM is consistent with previous findings [29]. As discussed previously, a decrease in oligodendrocyte density is not the only possible mechanism that could account for decreased or disrupted connectivity in this disorder.

The anterior corpus callosum connects both prefrontal cortices, also implicated in SZ, BPD and MDD, and the ACC is also important as an integrative area of the limbic system, involved in emotional processing. Disruption in these areas is consistent with the symptoms commonly reported in SZ.

Confounding factors

The cases of bipolar disorder had a longer mean PM delay than the cases from the other diagnostic groups. This was predominantly due to three male bipolar cases, numbers 32 (89 h), 34 (91 h) and 45 (100 h). However, this had no effect on the observed astrocyte or oligodendrocyte density.

The depression group showed a reduced age of death, which may reflect a higher number of suicides amongst this group. Similarly male schizophrenics showed a younger age of death than female schizophrenics, which was likely related to a higher number of suicides. However, these had no effects on the densities of either glial cell type measured.

Methodology

The use of 10-μm sections relies on a two-dimensional counting technique for cell density counts. This method has been the source of some controversy in contrast to three-dimensional stereological methods (see [2] for "Discussion"). Stereological methods may be more reliable for the measurement of absolute cell number, whereas using a two-dimensional direct comparison between identified disease states allows discriminative measurement of the different group cell densities. However, the consistency of these findings with others publications for both oligodendrocytes and GFAP mRNA [29, 33] suggest that multiple methods may be equally useful as long as rigorous controls and scientific principles are applied.

GFAP is a well-established stain for astrocytes, which made identification relatively easy when stained bodies of the appropriate size were observed with nuclei and/or with processes. More recent evidence from genechip arrays in transgenic mouse glia suggest that GFAP may not be expressed in all astrocytes [7], meaning either that GFAP-containing astrocytes may be decreased in the SCC of SZ, or are not producing GFAP in SZ. A future study would be useful to distinguish these points.

Antibodies for oligodendrocyte identification (CNPase and NOGO) did not stain with the clarity GFAP has in astrocytes; a problem commonly found in formalin-fixed paraffin-embedded tissue. Therefore, we used a combination of light cresyl stain with a moderate haematoxylin counterstain. The cresyl violet is a good general stain for histology, but the combination with the haematoxylin makes oligodendrocytes stand out more clearly, as the distinctly shaped and relatively large nucleus and small amount of cytoplasm these cells contain means they darken far more than other cell types with this combination of stains.

Conclusion

A decrease in astrocyte density could affect the functioning of the primary cingulate gyrus and the anterior corpus callosum as astrocytes are involved in cell firing and regulation of oligodendrocyte function. A decrease in astrocyte activity may reflect abnormal function and myelination in these areas, although the lack of change in oligodendrocyte density suggests that abnormal myelination may not be the underlying cause of anterior cingulate dysfunction. Recently, astrocytic D-serine has been shown to regulate neuronal long-term potentiation and regulates NMDA receptor-dependant plasticity in local synapses [20]. This suggests a possible link between the decreased astrocyte density observed in the SCC in SZ, and the suggested decreased function or output of that structure.

The nature of neuropathological studies prevents us from concluding whether changed glial densities are a causative factor or a result of SZ. Further studies need to

investigate the level of gliosis in high-risk individuals or examine the levels of gliotic markers *in vivo*.

Neuropathological studies of other brain regions implicated in these disorders are needed to determine whether the changes in astrocyte density, in contrast to overall levels of glial and relative to other glial cell types, are confined to the cingulate cortex and anterior corpus callosum or whether there is a wider involvement.

Acknowledgments The authors would like to thank Prof. Manuel Graeber and Dr. Federico Roncaroli for help with the histology and staining, Dr. Federico Turkheimer for advice on statistics, Dr. Dawn Duke for help with the data analysis and Dr. Andrew Dwork of Columbia University for comments on the manuscript. This work was funded by the Stanley foundation. The tissue was obtained from the Corsellis collection, which is supported by the Starr foundation and the West London Mental Health Trust.

References

1. Bechara A, Damasio H, Tranel D, Damasio AR (1997) Deciding advantageously before knowing the advantageous strategy. Science 275:1269–1272
2. Benes FM, Lange N (2001) Two-dimensional versus three-dimensional cell counting: a practical perspective. Trends Neurosci 24:11–17
3. Benes FM, McSparren J, Bird ED, SanGiovanni JP, Vincent SL (1991) Deficits in small interneurons in prefrontal and cingulate cortices of schizophrenic and schizoaffective patients. Arch Gen Psychiatry 48:996–1001
4. Botteron KN, Raichle ME, Drevets WC, Heath AC, Todd RD (2002) Volumetric reduction in left subgenual prefrontal cortex in early onset depression. Biol Psychiatry 51:342–344
5. Bouras C, Kövari E, Hof PR, Riederer BM, Giannakopoulos P (2001) Anterior cingulate cortex pathology in schizophrenia and bipolar disorder. Acta Neuropathol (Berl) 102:373–379
6. Bush G, Vogt BA, Holmes J, Dale AM, Greve D, Rosen LA (2002) Dorsal anterior cingulate cortex: a role in reward-based decision making. PNAS USA 99:523–528
7. Cahoy JD, Emery B, Kaushal A, Foo LC, Zamanian JL, Christopherson KS, Xing Y, Lubischer JL, Krieg PA, Krupenko SA, Thompson WJ, Barres BA (2008) A transcriptome database for astrocytes, neurons, and oligodendrocytes: a new resource for understanding brain development and function. J Neurosci 28:264–278
8. Carter CS, MacDonald AM, Botvinick M, Ross LL, Stenger VA, Noll D, Cohen JD (2000) Parsing executive processes: strategic vs. evaluative functions of the anterior cingulate cortex. PNAS USA 97:1944–1948
9. Carter CS, Mintun M, Nichols T, Cohen JD (1997) Anterior cingulate gyrus dysfunction and selective attention deficits in schizophrenia: [15O]H2O PET study during single-trial Stroop task performance. Am J Psychiatry 154:1670–1675
10. Chana G, Landau S, Beasley C, Everall IP, Cotter D (2003) Two-dimensional assessment of cytoarchitecture in the anterior cingulate cortex in major depressive disorder, bipolar disorder, and schizophrenia: evidence for decreased neuronal somal size and increased neuronal density. Biol Psychiatry 53:1086–1098
11. Cotter D, Hudson L, Landau S (2005) Evidence for orbitofrontal pathology in bipolar disorder and major depression, but not in schizophrenia. Bipolar Disord 7:358–369
12. Cotter D, Mackay D, Landau S, Kerwin R, Everall I (2001) Reduced glial cell density and neuronal size in the anterior cingulate cortex in major depressive disorder. Arch Gen Psychiatry 58:545–553
13. Devinsky O, Morrell MJ, Vogt BA (1995) Contributions of anterior cingulate cortex to behaviour. Brain 118:279–306
14. Drevets WC, Price JL, Simpson JR Jr, Todd RD, Reich T, Vannier M, Raichle ME (1997) Subgenual prefrontal cortex abnormalities in mood disorders. Nature 386:824–827
15. Eastwood SL, Harrison PJ (2001) Synaptic pathology in the anterior cingulate cortex in schizophrenia and mood disorders. A review and a Western blot study of synaptophysin, GAP-43 and the complexins. Brain Res Bull 55:569–578
16. Falkai P, Honer WG, David S, Bogerts B, Majtenyi C, Bayer TA (1999) No evidence for astrogliosis in brains of schizophrenic patients. A post-mortem study. Neuropathol Appl Neurobiol 25:48–53
17. Hakak Y, Walker JR, Li C, Wong WH, Davis KL, Buxbaum JD, Haroutunian V, Fienberg AA (2001) Genome-wide expression analysis reveals dysregulation of myelination-related genes in chronic schizophrenia. Proc Natl Acad Sci USA 98:4746–4751
18. Haznedar MM, Buchsbaum MS, Luu C, Hazlett EA, Siegel BV Jr, Lohr J, Wu J, Haier RJ, Bunney WE Jr (1997) Decreased anterior cingulate gyrus metabolic rate in schizophrenia. Am J Psychiatry 154:682–684
19. Heckers S, Heinsen H, Heinsen YC, Beckmann H (1990) Limbic structures and lateral ventricle in schizophrenia. A quantitative postmortem study. Arch Gen Psychiatry 47:1016–1022
20. Henneberger C, Papoulin T, Oliet SHR, Rusakov DA (2010) Long-term potentiation depends on release of D-serine from astrocytes. Nature 463:232–236
21. Highley JR, Walker MA, Esiri MM, McDonald B, Harrison PJ, Crow TJ (2001) Schizophrenia and the frontal lobes: post-mortem stereological study of tissue volume. Br J Psychiatry 178:337–343
22. Kalus P, Senitz D, Lauer M, Beckmann H (1999) Inhibitory cartridge synapses in the anterior cingulate cortex of schizophrenics. J Neural Transm 106:763–771
23. Kubicki M, Westin CF, Nestor PG, Wible CG, Frumin M, Maier SE, Kikinis R, Jolesz FA, McCarley RW, Shenton ME (2003) Cingulate fasciculus integrity disruption in schizophrenia: a magnetic resonance diffusion tensor imaging study. Biol Psychiatry 54:1171–1180
24. Miguel-Hidalgo JJ, Wei J, Andrew M, Overholser JC, Jurjus G, Stockmeier CA, Rajkowska G (2002) Glia pathology in the prefrontal cortex in alcohol dependence with and without depressive symptoms. Biol Psychiatry 52:1121–1133
25. Öngür D, Drevets WC, Price JL (1998) Glial reduction in the subgenual prefrontal cortex in mood disorders. PNAS USA 95:13290–13295
26. Rajkowska G, Miguel-Hidalgo JJ, Makkos Z, Meltzer H, Overholser J, Stockmeier C (2002) Layer-specific reductions in GFAP-reactive astroglia in the dorsolateral prefrontal cortex in schizophrenia. Schizophr Res 57:127–38; Erratum in: (2003) Schizophr Res 60:103
27. Roberts GW, Colter N, Lofthouse R, Bogerts B, Zech M, Crow TJ (1986) Gliosis in schizophrenia: a survey. Biol Psychiatry 21:1043–1050
28. Roberts GW, Colter N, Lofthouse R, Johnstone EC, Crow TJ (1987) Is there gliosis in schizophrenia? Investigation of the temporal lobe. Biol Psychiatry 22:1459–1468
29. Segal D, Schmitz C, Hof PR (2009) Spatial distribution and density of oligodendrocytes in the cingulum bundle are unaltered in schizophrenia. Acta Neuropathol 117:385–394
30. Todtenkopf MS, Vincent SL, Benes FM (2005) A cross-study meta-analysis and three-dimensional comparison of cell counting

in the anterior cingulate cortex of schizophrenic and bipolar brain. Schizophr Res 73:79–89
31. Wang F, Sun Z, Cui L, Du X, Wang X, Zhang H, Cong Z, Hong N, Zhang D (2004) Anterior cingulum abnormalities in male patients with schizophrenia determined through diffusion tensor imaging. Am J Psychiatry 161:573–575
32. Webster MJ, Knable MB, Johnston-Wilson N, Nagata K, Inagaki M, Yolken RH (2001) Immunohistochemical localization of phosphorylated glial fibrillary acidic protein in the prefrontal cortex and hippocampus from patients with schizophrenia, bipolar disorder, and depression. Brain Behav Immun 15:388–400
33. Webster MJ, O'Grady J, Kleinman JE, Weickert CS (2005) Glial fibrillary acidic protein mRNA levels in the cingulate cortex of individuals with depression, bipolar disorder and schizophrenia. Neuroscience 133:453–461
34. Wright IC, Rabe-Hesketh S, Woodruff PW, David AS, Murray RM, Bullmore ET (2000) Meta-analysis of regional brain volumes in schizophrenia. Am J Psychiatry 157:16–25
35. Yucel M, Pantelis C, Stuart GW, Wood SJ, Maruff P, Velakoulis D, Pipingas A, Crowe SF, Tochon-Danguy HJ, Egan GF (2002) Anterior cingulate activation during Stroop task performance: a PET to MRI coregistration study of individual patients with schizophrenia. Am J Psychiatry 159:251–254